

Spontaneous crumpling of active spherical shells

M. C. Gandikota¹, Shibananda Das^{1,2} and A. Cacciuto^{1*}

¹ *Department of Chemistry, Columbia University
3000 Broadway, New York, NY 10027*

² *Department of Polymer Science and Engineering,
University of Massachusetts,
Amherst, Massachusetts 01003*

The existence of a crumpled phase for self-avoiding elastic surfaces was postulated more than three decades ago using simple Flory-like scaling arguments. Despite much effort, its stability in a microscopic environment has been the subject of much debate. In this Letter we show how a crumpled phase develops reliably and consistently upon subjecting a thin spherical shell to active fluctuations. We find a master curve describing how the relative volume of a shell changes with the strength of the active forces, that applies for every shell independent of size and elastic constants. Furthermore, we extract a general expression for the onset active force beyond which a shell begins to crumple. Finally, we calculate how the size exponent varies along the crumpling curve.

It is well known that the energy cost required to deform an elastic surface is well accounted for by a bending and a stretching energy term [1–3]. Despite its apparent simplicity, the coupling between bending and stretching modes of deformation is highly nonlinear for thin elastic materials such as sheets and shells giving rise to mechanical behavior that is hard to predict. What makes these materials particularly exciting is that the ratio between stretching, E_s , and bending, E_b , energies for an arbitrary deformation of amplitude h on a surface of thickness t scales as $E_s/E_b \simeq (h/t)^2$ [1]. Therefore, for sufficiently thin surfaces, ($t \ll h$), only stretch-free deformations are allowed. Skin wrinkling under applied stress [4, 5], stress focusing via cone formation of crumpled paper [6], and buckling of thin shells [7], are just a few examples arising from this global constraint.

The theory of elasticity developed for continuum mechanics has been successfully used to study a number of microscopic systems, including viral capsids [8], graphite-oxide [9, 10] and graphene sheets [11, 12], cross polymerized membranes [13] and gels [14], the spectrin-actin network forming the cytoskeleton of red blood cells [15, 16] and close-packed nanoparticle arrays [17]. Significantly, at this length-scale, the nonlinear coupling between the different elastic modes can also be induced by thermal fluctuations with significant consequences for the structure of microscopic surfaces. For instance, it has been recently shown that large thermal fluctuations acting on thin spherical shells can result in an effective negative internal pressure capable of buckling the shell [18]. It has also been shown that thermal fluctuations renormalize the bending rigidity of thin elastic sheets which become stiffer as their size increases [19–21] leading to the stabilization of a flat phase for two-dimensional unsupported surfaces.

Simple Flory-like arguments [22] that work so well in establishing the scaling laws of self-avoiding polymers [23], predict that self-avoiding elastic sheets should be found in a crumpled state for negligible bending

rigidities. This state is characterized by the scaling of the radius of gyration of the sheet, R_g , with its side length, L , of the form $R_g \sim L^\nu$ with the Flory exponent $\nu = 4/5$ [24, 25]. Yet, numerical simulations of fully crystalline, self-avoiding elastic sheets indicate that these surfaces always acquire a rough, but overall extended (flat), state with a size exponent along their longitudinal directions $\nu \simeq 1$, even in the absence of bending rigidity (see for instance [26–29]). As of today, it is fair to say that the existence of a crumpled phase for large crystalline membranes in equilibrium remains uncertain.

Inspired by early experiments of graphite-oxide sheets in poor solvent [30] which seemed to indicate the presence of a crumpled phase upon improving the quality of the solvent, simulations were performed to include the presence of attractive interactions, but the crumpled phase was not observed [29]. Interestingly, thin elastic spherical shells in the presence of explicit attractive forces were initially reported to have a Flory exponent compatible with a crumpled phase in a temperature window that falls between the flat and the compact regimes [31], but simulations with larger shells did not find such intermediate regime [32]. For a comprehensive review on the subject, we refer the reader to references [3, 18, 22, 28, 33]. What is certain at this point is that the one way to reliably obtain a crumpled phase out of elastic thin surfaces is by quickly compressing them using a large external force [34–37], or by rapidly dehydrating graphene-oxide nanopaper [38].

In this Letter, we reconsider this problem within the framework of active matter, and study the effect of active, non-equilibrium fluctuations on the structure of a thin spherical shell. Crucially, we show how a crumpled phase, develops systematically and reliably for sufficiently large active forces. While a significant amount of work has been done to understand the structural and dynamic properties of active linear and ring polymers [39–44], and more recent work considered the behavior of fluid vesicles in the presence of active fluctuations or active

agents [45–49], apart from a few recent papers [50–52], very little is known about how elastic surfaces respond to non-equilibrium fluctuations, and this is an important problem given their relevance to biological and synthetic materials [53–55].

Numerical Model.—We model the thin spherical shell using a triangulated network of harmonic bonds [56] organized as an icosadeltahedron [57]. All vertices in icosadeltahedra are six-coordinated apart from twelve five-coordinated vertices (disclinations) as required by topological constraints. This structure are characterized by two integers (h, k) which define the relative position on the spherical lattice of the disclinations, and set the total number of vertices to $N = 10(h^2 + hk + k^2) + 2$. Although most of our data are obtained with this crystalline structure, we also considered amorphous spheres where the distribution of nodes on the sphere is disordered. The rest shape of the crystalline shell is an icosahedron [8] while that for an amorphous shell is a sphere [58].

To enforce self-avoiding interactions, we place a spherical particle of diameter σ at each vertex. Each of these vertex particles are connected to their nearest neighbors with a harmonic potential. The interaction potential of the system can be written as

$$U = K \sum_{\langle ij \rangle} (r_{ij} - \sigma)^2 + \kappa \sum_{\langle lm \rangle} (1 - \boldsymbol{\eta}_l \cdot \boldsymbol{\eta}_m) + 4\varepsilon \sum_{ij} \left[\left(\frac{\sigma}{r_{ij}} \right)^{12} - \left(\frac{\sigma}{r_{ij}} \right)^6 + \frac{1}{4} \right], \quad (1)$$

where r_{ij} is the distance between any two vertices i, j . The first term accounts for the harmonic bonds between nearest neighbor particles with a spring constant K . The second term is the bending energy where, κ is the bending rigidity of the shell and $(\boldsymbol{\eta}_l, \boldsymbol{\eta}_m)$ are the normal vectors of any two adjacent triangles, l and m , sharing an edge. The third term implements the excluded volume interactions between the vertex particles. The potential is cut off at $2^{1/6}\sigma$ and set to zero beyond that distance. Unless otherwise specified, we set $K = 160 k_B T_0 / \sigma^2$, $\kappa = 10 k_B T_0$, and $\varepsilon = k_B T_0$, where k_B is the Boltzmann constant and T_0 is the reference temperature. Activity is introduced in the system by adding a self-propelling velocity of constant magnitude v_p to each of the node particles. The system dynamics is resolved using Brownian motion according to

$$\begin{aligned} \frac{d\mathbf{r}_i(t)}{dt} &= \frac{1}{\gamma} \mathbf{f}_i + v_p \hat{\mathbf{n}}_i(t) + \sqrt{2D} \boldsymbol{\xi}(t), \\ \frac{d\hat{\mathbf{n}}_i(t)}{dt} &= \sqrt{2D_r} \boldsymbol{\xi}_r(t) \times \hat{\mathbf{n}}_i(t), \end{aligned} \quad (2)$$

where i is the particle index and the unit vector $\hat{\mathbf{n}}$ is the axis of propulsion. The conservative forces on each particle are denoted by $\mathbf{f}_i = -\partial U / \partial \mathbf{r}_i$. The translational diffusion coefficient D , temperature T_0 and the trans-

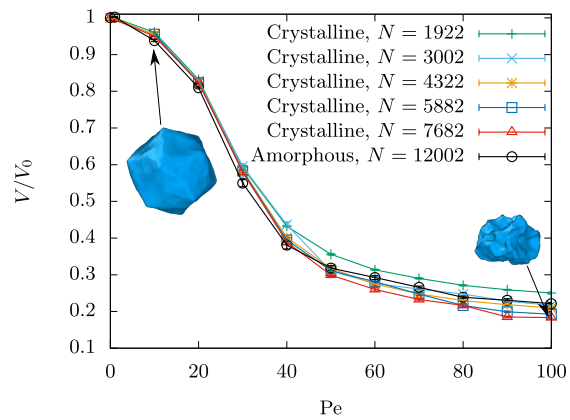


FIG. 1. The monotonically decreasing normalized volume (V/V_0) as a function of the activity Pe , for shells of different size, N and different structure (Crystalline/Amorphous). Simulation snapshots for the crystalline shell with $N = 7682$ are shown at $Pe = 10$ and $Pe = 100$. The elastic constants for all membranes are set to $K = 160 k_B T_0 / \sigma^2$ and $\kappa = 10 k_B T_0$.

lational friction γ are constrained to follow the Stokes-Einstein relation $D = k_B T_0 \gamma^{-1}$. Likewise, the rotational diffusion coefficient is constrained to be $D_r = k_B T_0 \gamma_r^{-1}$, with $D_r = 3D\sigma^{-2}$. The Gaussian white-noise terms induced by the solvent for the translational $\boldsymbol{\xi}$ and rotational $\boldsymbol{\xi}_r$ motions are characterized by the relations $\langle \boldsymbol{\xi}(t) \rangle = 0$ and $\langle \xi_p(t) \xi_q(t') \rangle = \delta_{pq} \delta(t - t')$ (here the indices p and q stand for the Cartesian components x, y, z).

The simulations have been carried out using the numerical package LAMMPS [59] and the units of length, time and energy respectively are set to be σ , $\tau = \sigma^2 D^{-1}$ and $k_B T_0$. All simulations were run with a time step smaller than $\Delta t = 2 \times 10^{-6} \tau$. The strength of the active forces is quantified by the Péclet number defined as $Pe = v_p \sigma / D$.

Crumpling of shells.— With the chosen set of parameters, our crystalline shell acquires a well-defined icosahedral state when thermalized in the absence of active fluctuations. This is expected given that with our parameters, the Föppl-von Kármán number $\gamma_F = \frac{4}{3} K R^2 / \kappa \gg 10^2$ [8] for every shell size considered in this study, $N \in [1922, 12002]$. We begin our analysis by monitoring the volume of the shell as a function of increasing values of the strength of the active forces. For small values of Pe , the shells develop smooth surface undulations on the scale of the shell radius without altering its overall shape. Upon increasing the activity, these undulations deepen resulting in a monotonically decreasing shell volume and a disruption of its global symmetry. For even larger Péclet numbers, the shell crumples to a volume that saturates at roughly 20% of its original value V_0 .

Interestingly, repeating the same calculations with different crystalline shell sizes $N \in [1922, 12002]$ and amorphous shells results in identical normalized volume V/V_0 curves. Figure 1 shows the results of this analysis. See

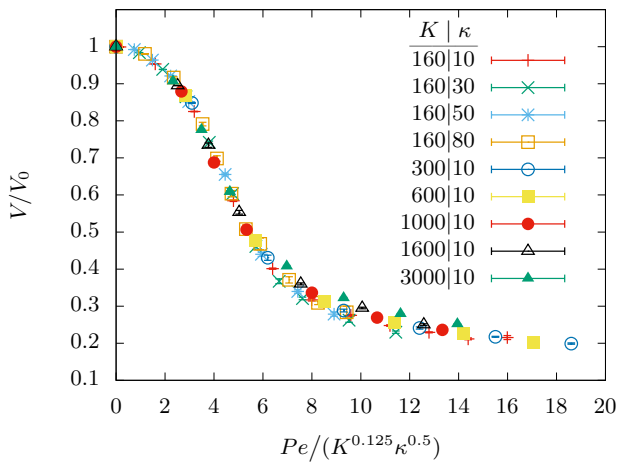


FIG. 2. The collapse of normalized volumes (V/V_0) as a function of $Pe/(K^{0.125}\kappa^{0.5})$ for various elastic spring constants K and bending constants κ . The size of the crystalline membrane here is $N = 4322$.

Fig.1 of S.I. for the cross-sections of both locally flat and crumpled spheres. We expect that the small systematic deviations in the crumpled state (for large Pe) are simply due to finite size effects. We find the flex of this curve, calculated by evaluating the maximum of $|dV/dPe|$, to be a reasonable estimator of the onset Péclet number, $Pe^* \approx 30$, beyond which the shells begin to crumple. Our results clearly show that the activity-induced crumpling of the shell is quite general and does not depend on the initial specific structure of the shell (crystalline or amorphous). We should also stress that the maximum of $|dV/dPe|$ does not show a diverging peak with system size, suggesting that for this system, crumpling is a smooth process devoid of singularities rather than a real phase transition.

To understand how the onset value, Pe^* , depends on the elastic parameters of the membrane, we performed the same calculations with different sets of stretching and bending rigidities, in the range of $K \in [160, 3000]$ and $\kappa \in [10, 80]$. Remarkably, as shown in Fig. 2, all data collapse into a master curve when we plot V/V_0 against $Pe/(K^{0.125}\kappa^{0.5})$. This suggests a universal crumpling onset for any shell size and any set of elastic constants beyond $Pe^* \simeq 5 K^{1/8}\kappa^{1/2}$. If the dependence on κ could be, in principle, rationalized by reinterpreting activity as an effective temperature generating fluctuations that carry an energy that scales as Pe^2 , and one would expect $Pe^2 > \kappa$, i.e. $Pe > \kappa^{1/2}$, for the shell to begin to crumple, this simple argument does not, however, explain the weaker dependence on the stretching constant. Furthermore, despite our best attempts, we were unable to use temperature to crumple our shells in equilibrium. Although, partial buckling of the shell can be achieved by increasing the temperature of the bath at equilibrium [18, 58], our simulations at high tempera-

tures show no crumpling of the shell. This holds true even when the temperature of the thermal bath is $100T_0$. At this temperature, even when we provide a crumpled shell as the initial configuration, the volume of the shell re-swells over-time to 60% of its original volume (see Fig.2 of S.I.). This suggests that the crumpled conformation of the shell is distinctly non-equilibrium in nature, and a simple temperature mapping of the activity is not sufficient to explain our data.

The Flory phase.—So far, we have used the term *crumpled* quite loosely and with the only intent of providing a visual description of the shape of the shell at large active forces. To accurately characterize the physical properties of this phase, we now calculate the size exponent, ν , for the shells deep into the crumpled phase. Using as a reference, the system with elastic constants discussed in Fig. 1, we set $Pe = 100$. We evaluate the size exponent by computing the shell structure factor $S(q)$ for different values of the shell radii $R \propto N^{1/2}$. We then plot $S(q)$ against qR^ν , and find the value ν for which all data points collapse onto the same curve within the range $2\pi/R_g$ and $2\pi/\sigma$. The results of this analysis are shown in Fig. 3. The best collapse is obtained for $\nu = 0.76(6)$, a result within error bars of the Flory exponent $\nu = 4/5$ predicted for the crumpled phase of self-avoiding membranes, and clearly different from $\nu = 1$ and $\nu = 2/3$ associated with the flat and the compact phase, respectively.

We also evaluated how the size exponent of the shell depends on the strength of the active forces along the full spectrum of the shape transformation. What we find is that the size exponent crosses over continuously from $\nu = 1$ in the icosahedral/spherical state, to $\nu = 0.76$

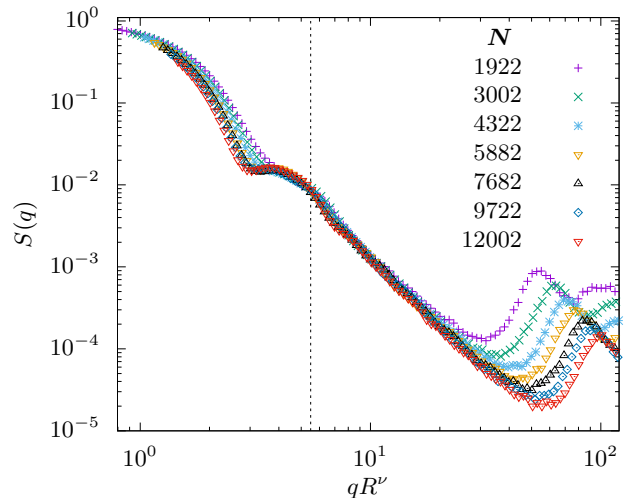


FIG. 3. Log-log plot of the structure factor $S(q)$ for different shell sizes N , at $Pe = 100$, as a function of the rescaled wave vector qR^ν . The best collapse of the data for $q > 2\pi/R_g$ is shown in this figure and is obtained for $\nu = 0.76 \pm 0.06$ which is within error bar of the Flory exponent $\nu = 4/5$.

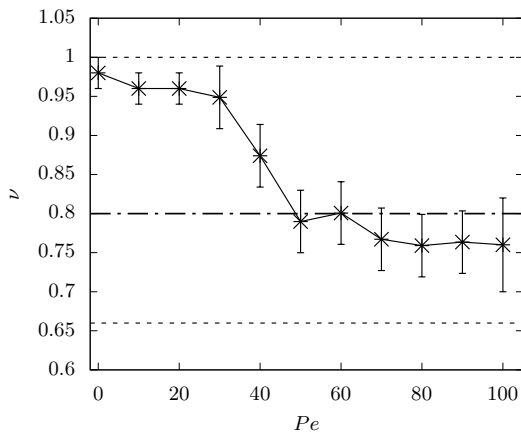


FIG. 4. Size-exponent of an elastic shell ν as a function of Péclet number Pe . The elastic constants here are $K = 160 k_B T_0 / \sigma^2$ and $\kappa = 10 k_B T_0$. The dotted lines indicate the size-exponents of a spherical ($\nu = 1$) and a compact ($\nu = 2/3$) phase, respectively. The dash-dotted line at $\nu = 4/5$ indicates the crumpled Flory phase. While the shell is locally flat for $Pe < Pe^* = 30$, the size-exponent for larger values of Pe show a clear departure from the locally flat phase. The size-exponent saturates to $\nu \approx 0.76$ for $Pe \gg Pe^*$.

in the collapsed state. We do observe somewhat faster change beyond $Pe = 30$ which we had identified as the onset Péclet number for crumpling. The results are shown in Fig. 4. Given the computational cost of these calculations, the values of ν in Fig. 4 for the largest values of Pe are obtained by collapsing the structure factor as discussed above using three curves (rather than seven) associated with spheres built from $N = 1922, 4322$ and $N = 7682$ vertices. We instead use a simple power law fit of the form $R_g(R) = aR^\nu$ to obtain the size exponent for values of Pe below 30 for which the shell has a simpler icosahedral shape.

Conclusions.— In this Letter, we carried out extensive numerical simulations to understand the role of active fluctuations on the structural properties of thin elastic shells. Remarkably, we observe that thin shells easily and fully crumple under the presence of active fluctuations. Furthermore, we discovered that for different elastic constants, the curves describing the relative volume change of the shells as a function of the strength of the active forces, collapse into a single universal curve when appropriately normalized. Along this curve, the size-exponent continuously decreases from $\nu = 1.00$ to $\nu = 0.76 \pm 0.06$, and the latter is compatible with the elusive crumpled phase postulated for self-avoiding elastic membranes.

It is known that sufficiently large thin spherical shells buckle due to an effective negative pressure generated by thermal fluctuations [18]. However, in the absence of an explicit internal pressure, we found no evidence of crumpling in such equilibrated shells even when the strength of the thermal fluctuations become comparable to that of the harmonic bonds that keep the shell together. This is

not surprising as a crumpled phase at such large temperatures would be entropically very unfavorable, suggesting that activity cannot be mapped into an effective temperature for thin spherical shells. This is a particularly intriguing result because we have recently shown [50] that active elastic sheets (rather than spherical shells) behave similarly to high temperature passive sheets [50]. Specifically, a crumpled phase was not found in that instance as the sheet remained extended for all Péclet numbers considered in that study. Our results thus raise questions about the role of topology and curvature in these systems.

We emphasize that, unlike the crumpled structures obtained by forced crumpling of quasi non-extensile surfaces such as paper or aluminium-foil, which remain static in a quenched disordered state [35–37], the crumpled phase of active shells continuously fluctuates among a large ensemble of crumpled configurations.

It is worth noting that studies of the one-dimensional analogs of our system, active rings in two dimensions, present a re-entrant behavior of the radius of gyration with activity. In that case, a narrow region for intermediate activities where the ring collapses has also been observed, but this is immediately followed by a re-swelling at larger activities [44]. We verified that re-swelling does not occur in our system by running a few simulations at larger activities $Pe = 200, 400$ (data not shown), making the two-dimensional shell qualitatively different than its lower dimensional counterpart.

More recently, the role of non-equilibrium fluctuations on the shape of an elastic shell has also been tested by performing Monte Carlo simulations with an explicit detail-balance breaking rule [52]. In this case, buckling of the shell was observed as a function of the degree of detail-balance breaking, but a crumpled phase was not observed.

A.C. acknowledges financial support from the National Science Foundation under Grant No. DMR-2003444.

* ac2822@columbia.edu

- [1] L. D. Landau, L. P. Pitaevskii, A. M. Kosevich, and E. M. Lifshitz, *Theory of Elasticity: Volume 7 (Theoretical Physics)* (Butterworth-Heinemann, Oxford, England, UK, 1986).
- [2] A. E. H. Love, *A Treatise on the Mathematical Theory of Elasticity (Dover Books on Engineering)* (Dover Publications, Mineola, NY, USA, 2011).
- [3] D. Nelson, S. Weinberg, and T. Piran, *Statistical Mechanics of Membranes and Surfaces (Second Edition)* (World Scientific Publishing Company, Singapore, 2004).
- [4] E. Cerda, K. Ravi-Chandar, and L. Mahadevan, *Nature* **419**, 579 (2002).
- [5] K. Efimenko, M. Rackaitis, E. Manias, A. Vaziri, L. Mahadevan, and J. Genzer, *Nat. Mater.* **4**, 293 (2005).
- [6] T. A. Witten, *Rev. Mod. Phys.* **79**, 643 (2007).

- [7] Th. Von Karman and H.-S. Tsien, *Journal of the Aeronautical Sciences* **7**, 43 (1939).
- [8] J. Lidmar, L. Mirny, and D. R. Nelson, *Physical Review E* **68**, 051910 (2003).
- [9] M. S. Spector, E. Naranjo, S. Chiruvolu, and J. A. Zasadzinski, *Phys. Rev. Lett.* **73**, 2867 (1994).
- [10] X. Wen, C. W. Garland, T. Hwa, M. Kardar, E. Kokufuta, Y. Li, M. Orkisz, and T. Tanaka, *Nature* **355**, 426 (1992).
- [11] S. Stankovich, D. A. Dikin, G. H. B. Dommett, K. M. Kohlhaas, E. J. Zimney, E. A. Stach, R. D. Piner, S. T. Nguyen, and R. S. Ruoff, *Nature* **442**, 282 (2006).
- [12] J. C. Meyer, A. K. Geim, M. I. Katsnelson, K. S. Novoselov, T. J. Booth, and S. Roth, *Nature* **446**, 60 (2007).
- [13] J. H. Fendler and P. Tundo, *Acc. Chem. Res.* **17**, 3 (1984).
- [14] P. C. Georges and P. A. Janmey, *J. Appl. Physiol.* (2005).
- [15] C. F. Schmidt, K. Svoboda, N. Lei, I. B. Petsche, L. E. Berman, C. R. Safinya, and G. S. Grest, *Science* **259**, 952 (1993).
- [16] S. E. Lux, *Blood* **127**, 187 (2016).
- [17] K. E. Mueggenburg, X.-M. Lin, R. H. Goldsmith, and H. M. Jaeger, *Nat. Mater.* **6**, 656 (2007).
- [18] A. Košmrlj and D. R. Nelson, *Physical Review X* **7**, 011002 (2017).
- [19] D. Nelson and L. Peliti, *Journal de physique* **48**, 1085 (1987).
- [20] J. A. Aronovitz and T. C. Lubensky, *Physical review letters* **60**, 2634 (1988).
- [21] P. M. Chaikin, T. C. Lubensky, and T. A. Witten, *Principles of condensed matter physics*, Vol. 10 (Cambridge university press Cambridge, 1995).
- [22] K. J. Wiese, “Phase transitions and critical phenomena,” (Elsevier, 2000) Chap. Polymerized membranes, a review, 1st ed.
- [23] P.-G. Gennes, *Scaling Concepts in Polymer Physics* (Cornell University Press, 1979).
- [24] K. J. Wiese, in *Phase transitions and critical phenomena Vol 19*, edited by C. Domb and J. L. Lebowitz (Elsevier, 2001) pp. 253–480.
- [25] M. Paczuski, M. Kardar, and D. R. Nelson, *Physical review letters* **60**, 2638 (1988).
- [26] M. Plischke and D. Boal, *Physical Review A* **38**, 4943 (1988).
- [27] F. F. Abraham and M. Kardar, *Science* **252**, 419 (1991).
- [28] M. J. Bowick, A. Cacciuto, G. Thorleifsson, and A. Travesset, *The European Physical Journal E* **5**, 149 (2001).
- [29] F. F. Abraham, W. Rudge, and M. Plischke, *Physical review letters* **62**, 1757 (1989).
- [30] X. Wen, C. W. Garland, T. Hwa, M. Kardar, E. Kokufuta, Y. Li, M. Orkisz, and T. Tanaka, *Nature* **355**, 426 (1992).
- [31] D. Liu and M. Plischke, *Physical Review A* **45**, 7139 (1992).
- [32] G. S. Grest and I. B. Petsche, *Physical Review E* **50**, R1737 (1994).
- [33] D. Nelson, T. Piran, and S. Weinberg, *Statistical mechanics of membranes and surfaces* (World Scientific, 2004).
- [34] Y. Kantor, M. Kardar, and D. R. Nelson, *Physical Review Letters* **60**, 238 (1988).
- [35] M. Gomes, *J. Phys. A* **20**, L283 (1987).
- [36] Y. Kantor, M. Kardar, and D. R. Nelson, *Physical Review A* **35**, 3056 (1987).
- [37] M. Gomes, T. Jyh, T. Ren, I. Rodrigues, and C. Furtado, *Journal of Physics D: Applied Physics* **22**, 1217 (1989).
- [38] X. Ma, M. R. Zachariah, and C. D. Zangmeister, *Nano letters* **12**, 486 (2012).
- [39] R. G. Winkler and G. Gompper, *J. Chem. Phys.* **153**, 040901 (2020).
- [40] S. Das and A. Cacciuto, *Phys. Rev. Lett.* **123**, 087802 (2019).
- [41] S. Das, N. Kennedy, and A. Cacciuto, *Soft Matter* **17**, 160 (2021).
- [42] M. C. Gandikota and A. Cacciuto, *Phys. Rev. E* **105**, 034503 (2022).
- [43] R. G. Winkler, J. Elgeti, and G. Gompper, *J. Phys. Soc. Jpn.* **86**, 101014 (2017).
- [44] S. M. Mousavi, G. Gompper, and R. G. Winkler, *The Journal of chemical physics* **150**, 064913 (2019).
- [45] P. Iyer, G. Gompper, and D. A. Fedosov, *Soft Matter* **18**, 6868 (2022).
- [46] F. Cagnetta, V. Škultéty, M. R. Evans, and D. Marenduzzo, *Phys. Rev. E* **105**, L012604 (2022).
- [47] H. Turlier and T. Betz, in *Physics of Biological Membranes* (Springer, Cham, Switzerland, 2018) pp. 581–619.
- [48] Y. Kulkarni, *J. Mech. Phys. Solids* **173**, 105240 (2023).
- [49] P. Iyer, G. Gompper, and D. A. Fedosov, *arXiv* (2023), 10.48550/arXiv.2301.07952, 2301.07952.
- [50] M. Gandikota and A. Cacciuto, *Soft Matter* **19**, 5328 (2023).
- [51] S. A. Mallory, C. Valeriani, and A. Cacciuto, *Phys. Rev. E* **92**, 012314 (2015).
- [52] V. Agrawal, V. Pandey, and D. Mitra, *arXiv preprint arXiv:2206.14172* (2022).
- [53] H. Turlier, D. A. Fedosov, B. Audoly, T. Auth, N. S. Gov, C. Sykes, J.-F. Joanny, G. Gompper, and T. Betz, *Nature physics* **12**, 513 (2016).
- [54] M. J. Bowick, N. Fakhri, M. C. Marchetti, and S. Ramaswamy, *Phys. Rev. X* **12**, 010501 (2022).
- [55] R. Kusters, C. Simon, R. L. Dos Santos, V. Caorsi, S. Wu, J.-F. Joanny, P. Sens, and C. Sykes, *bioRxiv*, 781153 (2019), 781153.
- [56] Y. Kantor and D. R. Nelson, *Phys. Rev. Lett.* **58**, 2774 (1987).
- [57] A. Šiber, *Symmetry* **12**, 556 (2020).
- [58] J. Paulose, G. A. Vliegenthart, G. Gompper, and D. R. Nelson, *Proceedings of the National Academy of Sciences* **109**, 19551 (2012).
- [59] S. Plimpton, *J. Comput. Phys.* **117**, 1 (1995).

APPENDIX

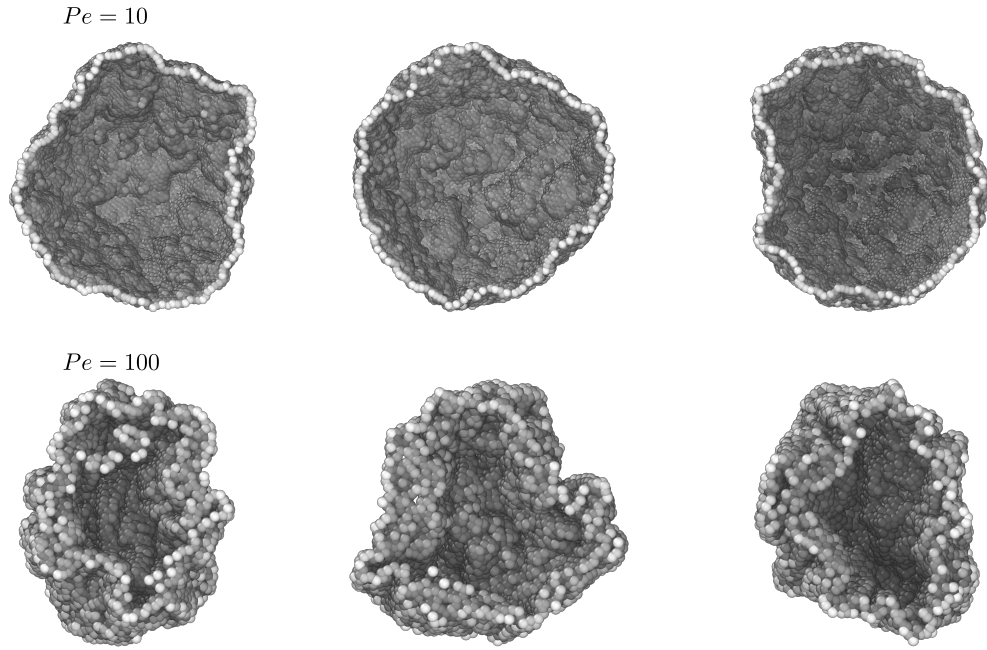


FIG. SI.1. Cross-sections of shells at $Pe = 10$ (top row) and $Pe = 100$ (bottom row). The perspectives are along three orthogonal axis. The images are for an amorphous shell of size $N = 12002$.

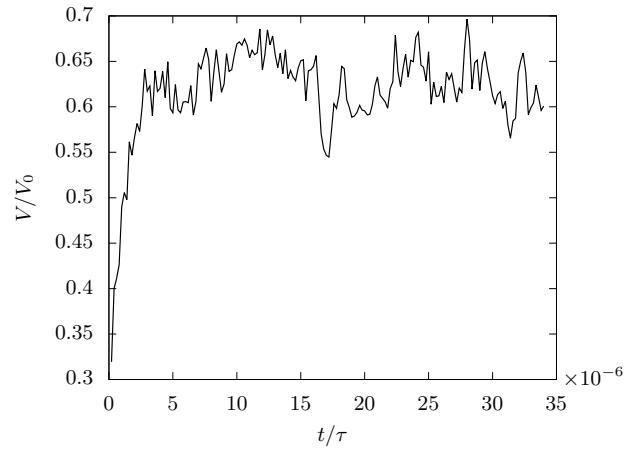


FIG. SI.2. Relative volume V/V_0 versus time depicting the re-swelling of a crumpled configuration. The initial configuration was generated by subjecting the shell to active fluctuations of strength $Pe = 100$ at $T = T_0$ after which the activity was removed while the temperature is increased to $T = 100T_0$. For this, we used an amorphous shell of size $N = 1922$.